Stem Cell Reports
Article

OPEN ACCESS

Expandable Arterial Endothelial Precursors from Human CD34$^+$ Cells Differ in Their Proclivity to Undergo an Endothelial-to-Mesenchymal Transition

Auston Z. Miller,[1] Alexander Satchie,[1] Alex P. Tannenbaum,[1] Aman Nihal,[1] James A. Thomson,[1,2,3] and David T. Vereide[1,*]

[1]Morgridge Institute for Research, Madison, WI 53715, USA
[2]Department of Cell and Regenerative Biology, University of Wisconsin School of Medicine and Public Health, Madison, WI 53706, USA
[3]Department of Molecular, Cellular, and Developmental Biology, University of California, Santa Barbara, CA 93106, USA
*Correspondence: dvereide@morgridge.org
https://doi.org/10.1016/j.stemcr.2017.12.011

SUMMARY

Arterial diseases continue to pose a major health concern but *in vitro* studies are limited because explanted cells can exhibit poor proliferative capacity and a loss of specificity. Here, we find that two transcription factors, *MYCN* and *SOX17*, induce and indefinitely expand in culture precursors of human arterial endothelial cells (expandable arterial endothelial precursors [eAEPs]). The eAEPs are derived from CD34$^+$ cells found in umbilical cord blood or adult bone marrow. Independent eAEP lines differ in their proclivity to undergo an endothelial-to-mesenchymal transition (EndoMT), a hallmark event in a broad array of vascular diseases and disorders. Some cell lines spontaneously become mesenchymal over time in culture, an effect exacerbated by inhibition of the fibroblast growth factor receptor, while others do not readily convert. These distinctions were exploited to identify genes that correlate with resistance to an EndoMT and to elucidate transcriptional changes that underpin the transition.

INTRODUCTION

Blood vessels comprise one of the largest organs; in humans they form a network that collectively stretches over 60,000 miles (Aird, 2005). This extensive plumbing is a prerequisite for sufficient oxygenation and nutrient supply for all other tissues of the body. Vascular tissue is composed of a luminal (intimal) layer of endothelial cells that, in small vessels, can be wrapped by support mural cells, or pericytes. In larger vessels, the endothelial cells are surrounded by an elastic smooth muscle layer that tends to be thicker in arteries than in veins. In the largest vessels, the smooth muscle layer is surrounded by an adventitial layer, a heterogeneous assembly of fibroblasts, immune cells (including lymphocytes, dendritic cells, and macrophages), and vascular progenitor cells (Stenmark et al., 2013).

During early development, endothelial cells arise from precursors known as angioblasts, which form vessels throughout the embryo and extra-embryonic tissues. After early development, endothelial progenitors have been found circulating in the blood, residing within the bone marrow, or residing within the blood vessel wall (Goligorsky and Salven, 2013; Kovacic et al., 2008). While much of the behavior of these cells remains to be elucidated, they are thought to produce endothelial progeny for the renewal or reconstruction of the vasculature throughout life.

Because the vascular system is essential for the maintenance of all other organs, it is not a surprise that cardiovascular diseases, particularly those arising in arterial vessels, are a leading cause of death worldwide (Lozano et al., 2012). In fact, studies of mummies from ancient societies indicate that vascular dysfunction has been an affliction of our species for thousands of years (Thompson et al., 2013). A prevalent malady is arteriosclerosis: the hardening or thickening of arteries. This disease process can involve the accumulation of fatty deposits within the vessel wall (atherosclerosis), hyperplasia of the intimal layer, and the deposition of calcium (Fishbein and Fishbein, 2015). Over time, arteriosclerosis gives rise to a wide array of debilitating to life-threatening conditions, including carotid, cerebral, coronary, peripheral, and renal artery diseases.

The cascade of events that leads to vascular disease tends to involve the dysfunction of multiple cell types, both those within the vascular tissue and those located in other organs, such as the liver or pancreas. The dysfunction that occurs in the arterial endothelium appears to involve a change of identity. The endothelial cells lose their endothelial characteristics and acquire the characteristics of cells found in connective tissue, such as fibroblasts or myofibroblasts, through a process called an endothelial-to-mesenchymal transition (EndoMT). This alteration appears to significantly contribute to atherosclerosis (Chen et al., 2015), fibrotic disorders (Piera-Velazquez et al., 2011), and vascular graft occlusion (Cooley et al., 2014).

To study the biology and pathology of human arterial endothelium, a common approach is to use cells isolated from cadaver arteries. However, these cells exhibit poor proliferative capacity *in vitro*, and methods to maintain their presumably more proliferative progenitors in culture have not yet been described. In addition, explanted

endothelial cells can lose their tissue-specific identity (Aird, 2007). In this study, we find that two transcription factors, *MYCN* and *SOX17*, induce and indefinitely expand in culture arterial endothelial precursors derived from CD34$^+$ progenitors purified from human umbilical cord blood or adult bone marrow. The precursors reveal distinct proclivities to undergo an EndoMT: some precursor cell lines are permissive for the transition while others are resistant. These differing properties were exploited to identify putative regulators of the EndoMT and examine the molecular mechanics of the transition. We believe the arterial endothelial precursors may be useful not only as tractable tools for biological or pathological studies but also as platforms for drug discovery.

RESULTS

MYCN and *SOX17* Induce and Expand Arterial Endothelial Precursors

We previously described an expandable hemangioblast (eHB) state induced in murine cells by six transcription factors: *Gata2*, *Lmo2*, *Mycn*, *Pitx2*, *Sox17*, and *Tal1* (Vereide et al., 2014). In that study, two of the factors, *Mycn* and *Sox17*, seemed to act synergistically as the principal drivers of indeterminate expansion, while the primary task of the remaining four factors was to promote a hemangioblast identity. The observation that *Mycn* and *Sox17* together drove expansion prompted us to consider other related cell types in which those two factors might enable expansion in culture. The pool of human CD34$^+$ progenitors found in bone marrow or umbilical cord blood (progenitors primarily specified for blood, endothelial, or mesenchymal fates) attracted our attention. Therefore, PiggyBac cassettes encoding doxycycline-inducible *MYCN* or *SOX17* along with a PiggyBac cassette encoding the doxycycline-responsive transactivator *Tet-On 3G* were introduced via electroporation into purified CD34$^+$ cells (Figures 1A and 1B). After culturing the electroporated cells for approximately 1 week in medium developed for endothelial cells supplemented with doxycycline (see Supplemental Experimental Procedures), discrete, adherent colonies of cells appeared and expanded (Figure 1C, images at 9 days post-electroporation) at a frequency of about one out of 250 transfected cells (Figure 1D). The cells appeared to be migratory, as they were often scattered about each colony (Figure 1C). At 9 days post-electroporation, colonies were only observed in wells containing cells in which both *MYCN* and *SOX17* were introduced (Figure 1D). After about 2 weeks, colonies with a different morphology could sometimes be observed to form in the presence of *MYCN* alone (data not shown, see Discussion) but were not observed to form in the presence of *SOX17* alone. Under the continued expression of the ectopic factors by the presence of at least 100 ng/mL doxycycline (Figure S1A), colonies induced by both *MYCN* and *SOX17* could be isolated, expanded, and established as cell lines. Of the established cell lines, the majority exhibited a normal karyotype (93%, 13 out of 14 lines tested; Table S1). A number of the cell lines exhibited an elongated cell morphology and doubled approximately every 1.5 days (Figures 1E and 1F). These cell lines expressed the endothelial markers CDH5 and PECAM1 and continued to express the markers as the ectopic factors were downregulated by reducing the concentration of doxycycline (Figures 1G, S1A, and S1B). In a similar fashion, the cell lines expressed an array of endothelial markers detected by RNA sequencing (RNA-seq), using non-endothelial vascular cells (pericytes and adventitial fibroblasts) as negative controls (Figure S1C). However, cells with abundant expression of ectopic *MYCN* and *SOX17* (100 ng/mL doxycycline) exhibited poor endothelial function: they failed to efficiently take up acetylated low-density lipoprotein (Ac-LDL) or form tubes in fibrin gels (Figures 1H, S2A, and S2B). In contrast, upon the downregulation of ectopic *MYCN* and *SOX17*, the cells displayed these functions (0 and 10 ng/mL doxycycline; Figures 1H, S2A, and S2B) while tending to reduce their proliferative capacity (Figure S2C) and exhibit a flatter morphology. In perfused fibrin gels, the cells could build large tubes, but the efficiency varied between cell lines (Figures 1I, 1J, S2D, and S2E). In the most efficient cell line, the tubes could grow to diameters in excess of 100 μm after a week under perfusion (Figures 1I and 1J). Together, these data indicate that *MYCN* and *SOX17* induce and expand endothelial precursors from human CD34$^+$ cells that give rise to functional endothelial cells upon the downregulation of the ectopic factors.

Expression analysis of markers preferentially associated with either venous or arterial endothelial cells indicated that the precursors and their mature progeny possessed an arterial identity (Figure 2A). Not only did the arterial markers tend to be more robustly expressed in these cells when compared with explanted, early passage human arterial endothelial cells but the venous markers tended to be more overtly downregulated. This observation is consistent with previous reports indicating that explanted endothelial cells tend to lose tissue-specific gene expression (Durr et al., 2004; Lacorre et al., 2004). Instead, the levels of the arterial markers in the mature endothelial cells derived from the precursors expanded by *MYCN* and *SOX17* were more comparable with the levels found in arterial endothelial cells freshly differentiated from pluripotent stem cells (Zhang et al., 2017). To confirm an arterial identity, the cells were tested in functional assays. In contrast with venous cells, which have previously been shown to efficiently recruit leukocytes in the presence of the inflammatory

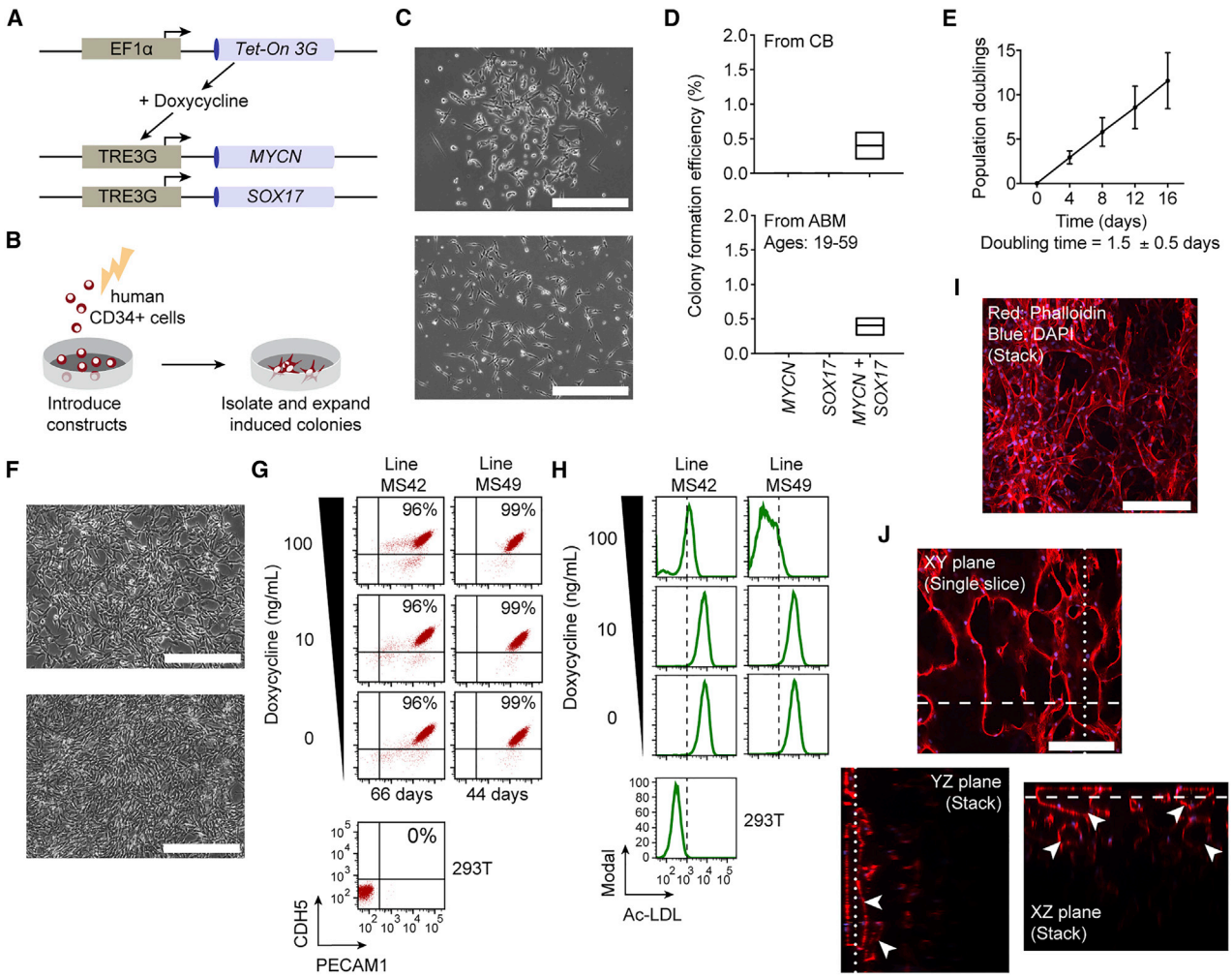

Figure 1. *MYCN* and *SOX17* Induce and Expand Endothelial Precursors

(A and B) Experimental approach. (A) Vectors used. Vectors were integrated in cells by the PiggyBac transposase. The promoter EF1α drives constitutive expression of *Tet-On 3G*. In the presence of doxycycline, Tet-On 3G binds the TRE3G promoter, upregulating expression of *MYCN* and *SOX17* (encoded on separate vectors). (B) The three vectors from (A) were introduced by electroporation into human $CD34^+$ cells (cultured for two days prior to electroporation). The electroporated cells were then cultured in the presence of doxycycline to induce colony formation and expansion.

(C) Example colonies arising 9 days after electroporation as described in (B). Phase-contrast images. Scale bars, 400 μm.

(D) Efficiencies of colony formation after 9 days. The boxes indicate the maximum to minimum efficiencies from at least two independent experiments; the horizontal lines within the boxes indicate the means. CB, cord blood; ABM, adult bone marrow. The range of the ages of the adult bone marrow donors is provided in years.

(E) Growth curve, results are the average ± SD from six independent cell lines, three derived from cord blood and three derived from adult bone marrow.

(F) Example phase-contrast images of endothelial precursor cell lines. Scale bars, 400 μm.

(G and H) Cell lines were maintained in culture by the ectopic expression of *MYCN* and *SOX17* (100 ng/mL doxycycline) and matured by downregulating the factors for 4 days (10 or 0 ng/mL doxycycline). 293T cells served as negative controls. Results are from two independent cell lines, one derived from cord blood and the other derived from adult bone marrow. (G) Analysis of the endothelial markers CDH5 and PECAM1 by flow cytometry. The number of days indicates the time in culture from the induction of the ectopic expression of *MYCN* and *SOX17*. (H) Analysis of the uptake of fluorescently labeled acetylated low-density lipoprotein (Ac-LDL) by flow cytometry.

(I and J) Tube formation. Cells were embedded in a fibrin gel and perfused for 7 days in the absence of doxycycline. Scale bars, 200 μm. (I) Maximum intensity projection of 100 Z-slices within the gel. (J) Left: single Z-slice image near the bottom of the gel in (I). The dotted or dashed lines indicate the positions in the bottom two images at which the YZ or XZ stacks (195 Z-slices from bottom to top of the gel) are viewed. Arrowheads point to lumen. See also Figures S1, S2, and Table S1.

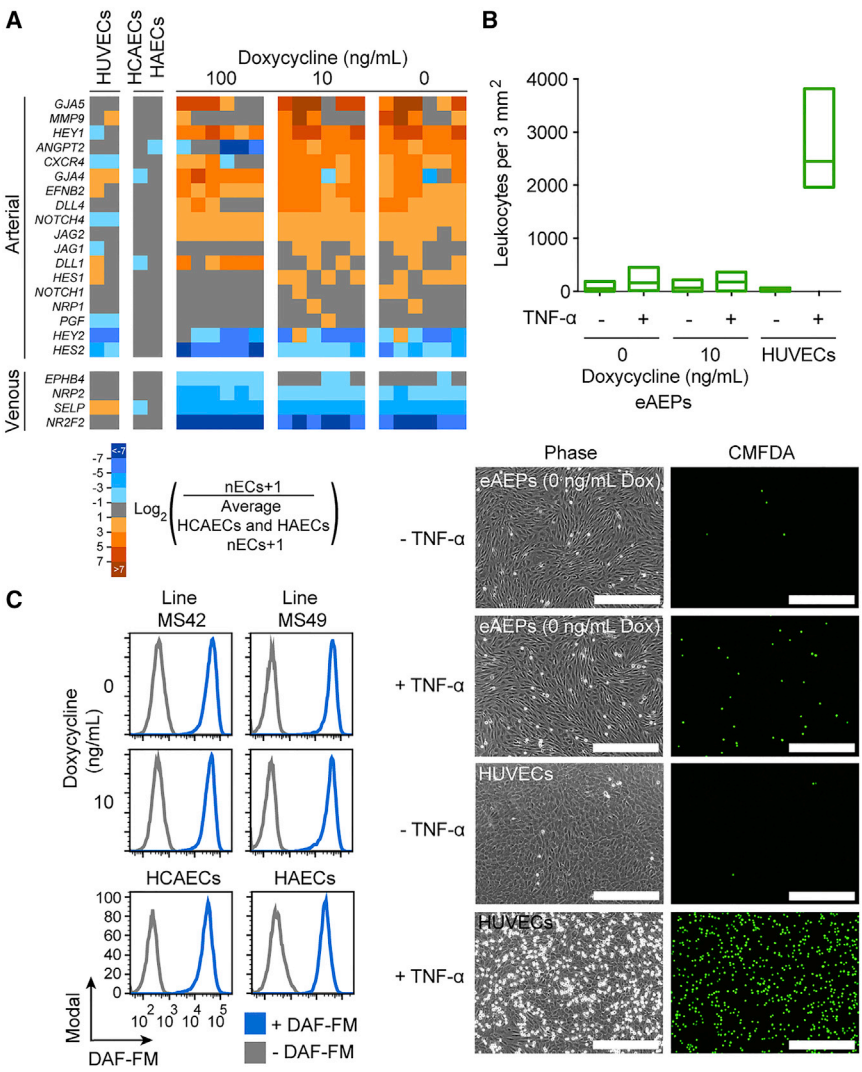

Figure 2. The Endothelial Precursors Possess an Arterial Identity

(A) Expression analysis by RNA-seq of arterial and venous markers, using samples from Figure S1C. The results are from six independent cell lines, three derived from cord blood and three derived from adult bone marrow, and controls (explanted endothelial cells). HAECs, human aortic endothelial cells; HCAECs, human coronary artery endothelial cells; HUVECs, human umbilical vein endothelial cells; nECs, normalized expected counts. The heatmap is depicted on $\log_2$ scale, using the average expression values (nECs + 1) of the HCAECs and HAECs as the baseline for comparison.

(B) Leukocyte recruitment assay. Cells were treated with 1 ng/mL TNF-α, incubated with U937 leukocytes (fluorescently labeled with CMFDA [5-chloromethylfluorescein diacetate]), and then rigorously washed. Top, quantification from six independent cell lines (the same cell lines as [A]), each tested side by side with HUVECs. The boxes indicate the maximum to minimum number of leukocytes detected; the horizontal lines within the boxes indicate the means. Bottom, example images. Scale bars, 400 μm.

(C) NO (nitric oxide) output assay. Cells were treated with DAF-FM, a cell-permeable dye that becomes fluorescent when exposed to NO, and analyzed by flow cytometry. Results are from two independent cell lines, one derived from cord blood and the other derived from adult bone marrow. Blue, treated; gray, untreated. (A–C) The endothelial precursors were maintained in culture by the ectopic expression of *MYCN* and *SOX17* (at least 100 ng/mL doxycycline). To allow maturation, cells were cultivated for 4 days with 0 or 10 ng/mL doxycycline. See also Figure S3.

cytokine tumor necrosis factor alpha (TNF-α) (Hauser et al., 1993), leukocytes were poorly recruited to the matured progeny of the precursors (Figure 2B). Furthermore, the cells efficiently produced nitric oxide as detected by the reporter 4-amino-5-methylamino-2′,7′-difluorofluorescein diacetate (DAF-FM) (Figures 2C and S3A), a capacity thought to be pronounced in arterial cells (Cicinelli et al., 1999). Lastly, the cells were subjected to different rates of fluid flow to mimic wall shear stress (WSS), the pressure exerted on the endothelium by the flow of blood. Because it is now clear that WSS varies markedly along the arterial tree, we chose conditions that mimic a moderate WSS (10 dyn/cm^2) measured in healthy humans (Cheng et al., 2007) as well as conditions that mimic regions under lower WSS at rest (1.5 dyn/cm^2), such as the infrarenal aorta (Cheng et al., 2003) or conditions that mimic higher WSS (30 dyn/cm^2). Depending on the precursor cell line, cells best aligned with the direction of the flow at 1.5, 10, or 30 dyn/cm^2 (Figures S3B and S3C). Collectively, these data indicate that (1) the precursors possess an arterial identity (thus we dubbed them "expandable arterial endothelial precursors" [eAEPs]) and (2) independently derived cell lines display functional distinctions, a fortuitous feature we subsequently exploited.

eAEPs Exhibit Different Proclivities to Undergo an EndoMT

The eAEP lines derived from either cord blood or bone marrow were cultured extensively, maintained in the precursor state by the expression of ectopic *MYCN* and

SOX17, with periodic maturation assays as described in Figure 1G. Over time in culture, some cell lines exhibited a marked reduction in the percentage of mature endothelial progeny efficiently expressing CDH5 and PECAM1 (Figure 3A, top two dot plots). In contrast, other cell lines continued to produce mature endothelial progeny with high levels of CDH5 and PECAM1 for much longer (Figure 3A, bottom two dot plots). To determine the identity of the cells expressing lower levels of CDH5 and PECAM1, cells from independent lines were sorted by fluorescence-activated cell sorting (FACS) for low, mid, and high levels of PECAM1 and then examined by RNA-seq. This analysis revealed a number of endothelial markers declining in expression along with PECAM1 (Figure 3B). In contrast, a majority of markers previously associated with an *in vivo* or *in vitro* transition of endothelial cells to a mesenchymal state (EndoMT) increased in expression as PECAM1 levels dropped. Together, these data indicate that some eAEP cell lines are more prone to a spontaneous EndoMT ("EndoMT-permissive") than others ("EndoMT-resistant").

Previous work has demonstrated that the fibroblast growth factor (FGF) pathway is a central regulator of the EndoMT; the forced disruption of FGF signaling prompts endothelial cells to transition (Chen et al., 2015). Guided by this observation, we developed a rapid assay to further investigate the differences among the eAEP cell lines. Precursors, maintained by the expression of ectopic *MYCN* and *SOX17*, were challenged for 4 days by the absence of FGF2 or the presence of the FGFR inhibitor PD173074 ("PD17"; Figures 3C and S4A). Following the 4-day challenge, the cells were then allowed to recover and mature. This approach highlighted differences among cell lines: the challenges exacerbated the transition of EndoMT-permissive eAEPs (lines MS15 and MS64) but poorly promoted the transition of EndoMT-resistant eAEPs (lines MS49 and MS53) (Figures 3D, S4B, and S4C). Exposure to transforming growth factor β (TGF-β), another previously identified inducer of an EndoMT (Kokudo et al., 2008), weakly augmented the transition of permissive cell lines but not the more resistant ones (Figures S4D and S4E). The mild effects seen with TGF-β treatment may be a result of the reduced expression of the TGF-β receptor *TGFBR2* and TGF-β co-receptors *ENG* and *TGFBR3* in the precursor state (100 ng/mL doxycycline) of permissive and resistant cell lines (Figure S1C and data not shown). Analysis of marker expression by RNA-seq, conducted on unsorted populations of cells, produced some mechanistic insight into the differences among cell lines. At the end of the 4-day challenge, all lines displayed some loss of endothelial markers and acquisition of mesenchymal ones (Figure 3E, compare day 4 samples). However, after recovery and maturation, these trends became even more pronounced for the permissive cell lines, while the resistant lines reversed the trends, appearing to rebound toward an endothelial identity (Figure 3E, compare day 8 samples). These data indicate that the distinctions among cell lines do not involve the ability to receive a mesenchymal-promoting signal. Rather, they appear to involve a threshold of commitment to the mesenchymal state that is higher in resistant cell lines than in permissive ones. Very late passage resistant lines show an increased sensitivity to PD17 (compare Figures S4D and S4F), and spontaneously transitioning cells could be isolated from one of the more resistant lines at very late passage (Figure 3B, right-most sample for each condition), indicating that the higher threshold of commitment observed in resistant cell lines is not completely fixed but instead can slowly lower with time.

An alternative explanation for the behavior of the EndoMT-permissive eAEP lines is that they arose as mixed populations from different founding cells, some of which were mesenchymal and simply outgrew the others over time or with the inhibition of the FGF pathway. To rule out this possibility, multiple experimental approaches were taken. First, we exploited the fact that the number of integrated vectors encoding *MYCN*, *SOX17*, or *Tet-On 3G* varies among independent cell lines, forming a molecular "signature" distinctive for each line (Figure S5A, top). Four EndoMT-permissive cell lines were cultivated with PD17 for up to 24 days to create populations of cells in which the large majority of the cells had lost an endothelial identity and acquired a mesenchymal one (Figure S5A, middle and bottom plots). The vector integration signature of these cells matched that of early passage control cells unperturbed with PD17 and mostly endothelial in nature. In a second approach, subclones of the permissive cell line MS15 were generated and challenged by PD17. The subclones readily underwent an EndoMT when challenged, in contrast with unchallenged controls (Figures S5B and S5C). In a third approach, eAEP cell lines were established by sorting single transfected $CD34^+$ cells from cord blood into wells by FACS; these cell lines also differed in their capacity to undergo an EndoMT (described in more detail below; Figure 5).

We assessed whether proclivity to an EndoMT correlated with different levels of the ectopic factors. First, the number of integrated vectors was examined (Figures S5D–S5F). Cell lines derived from adult bone marrow integrate significantly more vectors encoding *MYCN* than lines derived from cord blood (Figure S5D). To control for this effect, permissive and resistant cell lines arising from cells of the same origin were compared, and no significant differences were observed (Figure S5F). Furthermore, no significant differences in the expression of *Tet-On 3G* or the combined expression of ectopic and endogenous transcripts of *MYCN* and *SOX17* were found (Figures S5G and S5H). Taken together, these data indicate that

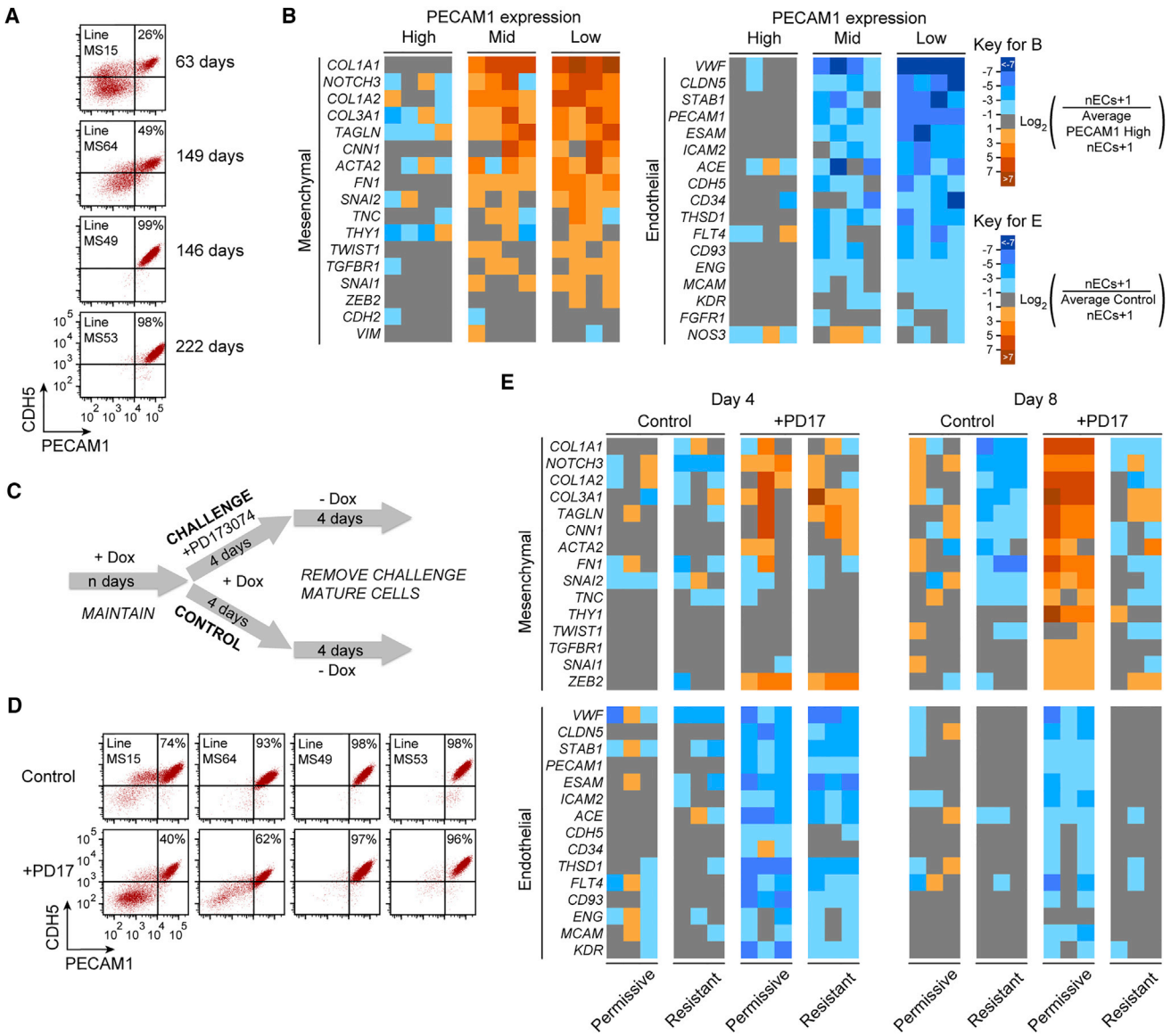

Figure 3. eAEPs Exhibit Different Proclivities to Undergo an Endothelial-to-Mesenchymal Transition

(A) Independent eAEP cell lines were maintained in culture by the ectopic expression of *MYCN* and *SOX17* (at least 100 ng/mL doxycycline) and then matured for 4 days by the withdrawal of doxycycline. Analysis of the endothelial markers CDH5 and PECAM1 by flow cytometry. The double-positive gate used here identifies cells with high expression of CDH5 and PECAM1, in contrast with the gate used in previous figures to identify all double-positive cells. The number of days indicates the time in culture from the induction of the ectopic expression of *MYCN* and *SOX17*.

(B) Four cell lines exhibiting decay of PECAM1 (three at early passage as exemplified in [A], two topmost dot plots; one at very late passage) were sorted by FACS for high, mid, or low PECAM1 expression and then analyzed by RNA-seq. nECs, normalized expected counts. The heatmap is depicted on $\log_2$ scale, using the average expression values (nECs + 1) of the PECAM1 high samples as the baseline for comparison.

(C) Experimental approach to exacerbate an EndoMT. The eAEPs, maintained with 100 ng/mL doxycycline, were challenged for 4 days with FGFR inhibitor PD173074 (PD17) and then allowed to recover and mature for 4 days in the absence of PD17, alongside controls never exposed to the inhibitor.

(D) Analysis by flow cytometry of the endothelial markers CDH5 and PECAM1 at the end (8 days) of the challenge experiment described in (C) using the same gate as in (A).

(E) RNA-seq analysis of the PD17 challenge described in (C). The heatmap is depicted on $\log_2$ scale, using the average expression values (nECs + 1) of the control samples (no PD17) as the baseline for comparison at each time point. See also Figures S4 and S5.

EndoMT-permissive eAEPs are intrinsically more prone to become mesenchymal than EndoMT-resistant ones.

Isolation of Cell Lines That Apparently Transition to a Mesenchymal State during Initial Establishment in Culture

A small subset of the precursor lines derived from cord blood or adult bone marrow CD34$^+$ cells, upon initial expansion in culture, exhibited a star-shaped morphology (Figure 4A) sometimes seen in EndoMT-transitioning eAEP lines. The cells expressed ectopic *MYCN* and *SOX17* at levels comparable with the levels detected in the eAEP lines (compare Figures S1A and 4B); however, they poorly expressed the vascular markers CDH5 and PECAM1 and tended to lose these markers with the downregulation of ectopic *MYCN* and *SOX17* or over extended time in culture (Figure 4C). The cell lines preferentially expressed a number of mesenchymal markers found in vascular mesenchymal cells (pericytes and adventitial fibroblasts) or in cells undergoing an EndoMT (Figure 4D). The mesenchymal markers often increased in expression as the ectopic factors were downregulated, in contrast with the endothelial markers. Thus, these cell lines appear to be highly permissive eAEPs, undergoing an EndoMT during their initial establishment in culture to become "expandable mesenchymal precursors" (eMPs). The eMP lines from cord blood tended to expand rapidly by doubling approximately every 0.7 days; their rate of expansion abated somewhat as the factors were shut off (Figures 4B and 4E) and the cells adopted a flatter, fibrotic morphology. Not all eMP lines rapidly expand in culture, however. For example, line MS51, derived from adult bone marrow, resembles the other eMP lines with respect to morphology, gene expression, and low levels of CDH5 and PECAM1, but it differs in that it expands slower in the presence of the ectopic factors, does not expand detectibly in their absence, and does not further lose the low level of CDH5 and PECAM1 as the ectopic vectors are shut off (Figures 4B, 4C, and 4F).

Comparison of the Levels of PROM1 on Founding CD34$^+$ Cells with Efficiency of eAEP Colony Formation and Proclivity to an EndoMT

Among the surface markers known to be expressed in the pool of CD34$^+$ progenitors from cord blood or bone marrow, the levels of the marker PROM1 (CD133) vary substantially among cells (Figure 5A) (Gorgens et al., 2013). Thus, we examined subpopulations of CD34$^+$ cells that expressed different levels of PROM1 for their capacity to give rise to EndoMT-permissive and EndoMT-resistant eAEPs. Cells were electroporated with vectors described in Figure 1 along with a non-integrating plasmid encoding GFP, allowed to recover overnight in the absence of doxycycline, and then sorted by FACS for those that were transfected (denoted by the expression of GFP) and displayed no, low, or high expression of PROM1 (Figure 5A). The sorted cells were then cultivated in 96-well plates in the presence of doxycycline and examined for the formation of eAEP colonies after 9 days. The eAEP colonies tended to form at higher efficiencies from PROM1$^-$ or PROM1^{low} fractions of CD34$^+$ cells from cord blood (Figure 5B, top), and to form marginally more efficiently in the PROM1^{low} fractions of CD34$^+$ cells from adult bone marrow. The experiments with cells from adult bone marrow were confounded, however, by a very low colony formation efficiency from sorted cells (approximately 10-fold lower than that observed from unsorted adult bone marrow cells; compare results in Figure 5B with those in Figure 1D). Colonies from each PROM1 fraction were expanded for the same number of days in culture and then examined for their capacity to spontaneously transition to a mesenchymal state. Both EndoMT-resistant eAEPs (those with greater than 90% of the cells expressing high levels of CDH5 and PECAM1) and EndoMT-permissive eAEPs (those with less than 90% of the cells expressing high levels of CDH5 and PECAM1) were observed to arise from each PROM1 fraction (Figures 5C and 5D). Together, these results indicate that, while CD34$^+$ cells with lower levels of PROM1 are more likely to give rise to eAEPs (at least those sourced from cord blood), the level of PROM1 on the founding cells does not correlate with the propensity of their daughter eAEPs to undergo an EndoMT.

The eAEPs Preferentially Originate from Hematopoietic Progenitors

Other markers of CD34$^+$ progenitors besides PROM1 were used to determine the origins of the eAEPs. For these experiments, only cord blood CD34$^+$ cells were examined. Colonies of eAEPs were found to preferentially form from cells sorted for high expression of CD45 (Figure 5E), suggesting they arose from hematopoietic progenitors. Thus, markers previously found to fractionate the pool of hematopoietic CD34$^+$ cells were used (Doulatov et al., 2010; Gorgens et al., 2013). While eAEP colonies were observed to arise from any of the fractions examined, they preferentially formed from cells that were CD45RA$^-$ and THY1$^-$ (Figures 5F and 5G). In addition, we did not detect any transfected cells markedly expressing FLT3 (CD135) (data not shown). The cells found to preferentially give rise to eAEP colonies (PROM1$^{low/-}$THY1$^-$CD45^{high}CD45RA$^-$) are the major subpopulation of the pool of transfected CD34$^+$ cells from cord blood (56%–67% of all transfected cells; Figure 5H). This subpopulation is enriched for progenitors that give rise to erythroid and myeloid cells (Doulatov et al., 2010; Gorgens et al., 2013) (see Discussion).

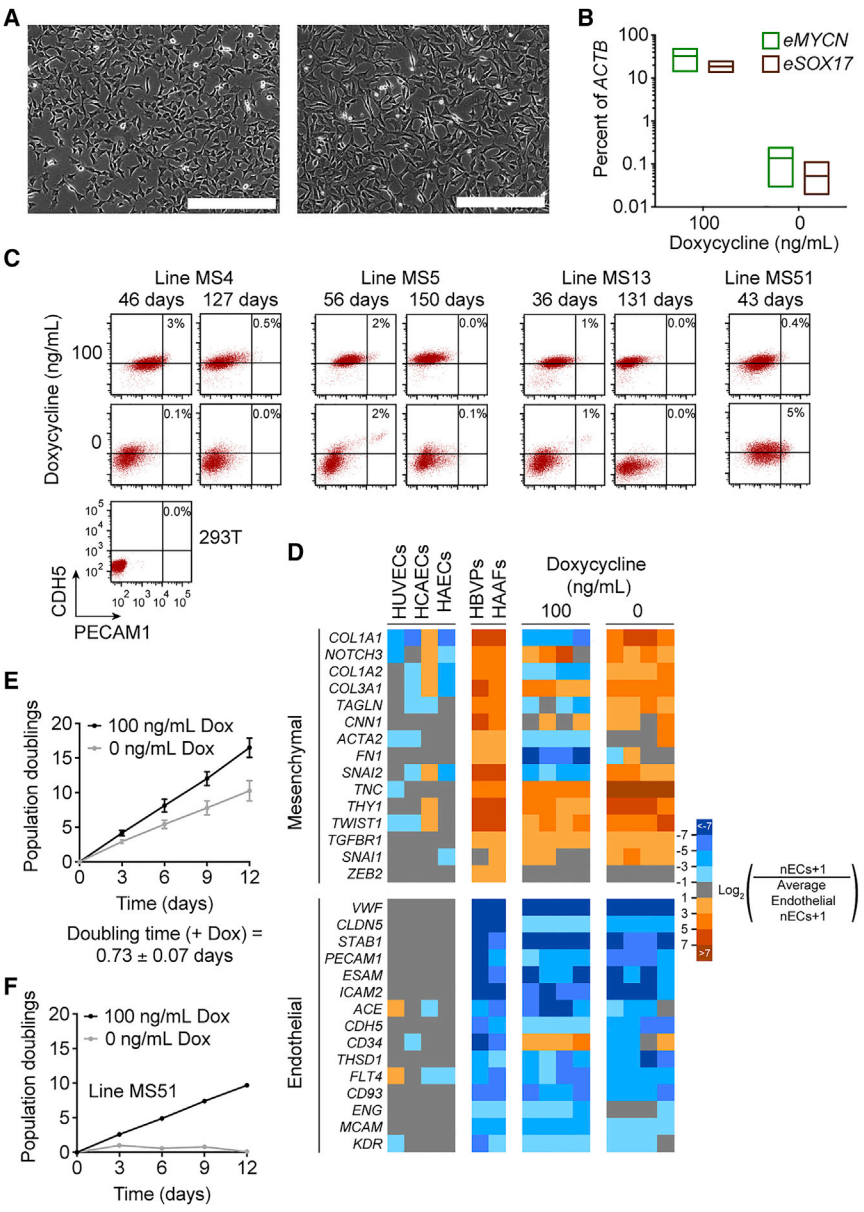

Figure 4. Some Cell Lines Induced by *MYCN* and *SOX17* are Mostly Mesenchymal upon Establishment in Culture

(A) Example phase-contrast images of mesenchymal precursor cell lines. Scale bars, 400 μm.

(B) Measurements by RT-qPCR of the expression levels of ectopic *MYCN* and *SOX17* (*eMYCN* and *eSOX17*). The boxes indicate the maximum to minimum values from four independent cell lines, three derived from cord blood and one derived from adult bone marrow; the horizontal lines within the boxes indicate the means. Values are normalized as a percentage of *ACTB* and presented on a $\log_{10}$ scale, with a threshold of detection cutoff of 0.01%.

(C) Analysis of the endothelial markers CDH5 and PECAM1 of the cell lines in (B) by flow cytometry. The double-positive gate used here identifies cells with high expression of CDH5 and PECAM1. The number of days indicates the time in culture from the induction of the ectopic expression of *MYCN* and *SOX17*. 293T cells served as negative controls.

(D) RNA-seq analysis of the cell lines in (B) using the control samples (explanted vascular cells) from Figure S1C. HAAFs, human aortic adventitial fibroblasts; HAECs, human aortic endothelial cells; HBVPs, human brain vascular pericytes; HCAECs, human coronary artery endothelial cells; HUVECs, human umbilical vein endothelial cells; nECs, normalized expected counts. The heatmap is depicted on $\log_2$ scale, using the average expression values (nECs + 1) of the HUVECs, HCAECs, and HAECs samples as the baseline for comparison.

(E) Growth curve; results are the average ± SD from three independent cell lines derived from cord blood.

(F) Growth curve for the line MS51, derived from adult bone marrow. (B–D) Cells were maintained in culture by the ectopic expression of *MYCN* and *SOX17* (at least 100 ng/mL doxycycline) and matured for 3 days by the withdrawal of doxycycline. See also Table S1.

eAEPs and eMPs Form a Distinct Transcriptional Topography That Reveals Insights into the EndoMT

Principal component analysis (PCA) of the transcriptomes of the different cell types described thus far, along with explanted vascular cells as controls, supported our findings well (Figure 6A). For example, eAEPs spontaneously transitioning to a mesenchymal state after time in culture track away from early passage EndoMT-permissive lines or EndoMT-resistant lines and toward the cluster of eMPs. The mature progeny of the eMPs group with explanted vascular mesenchymal cells (adventitial fibroblasts and pericytes). The transitioned progeny of eAEPs (sorted for mid or low levels of PECAM1 expression) also group with the mature mesenchymal cells, while the non-transitioned cells (sorted for high levels of PECAM1 expression) cluster with the mature progeny of early passage EndoMT-permissive lines or EndoMT-resistant lines and explanted vascular endothelial cells. A similar result was observed with unsupervised hierarchical clustering (Figure 6B).

We capitalized on the differing phenotypes presented by the eAEPs and eMPs to identify genes associated with an EndoMT in an arterial context. First, genes whose

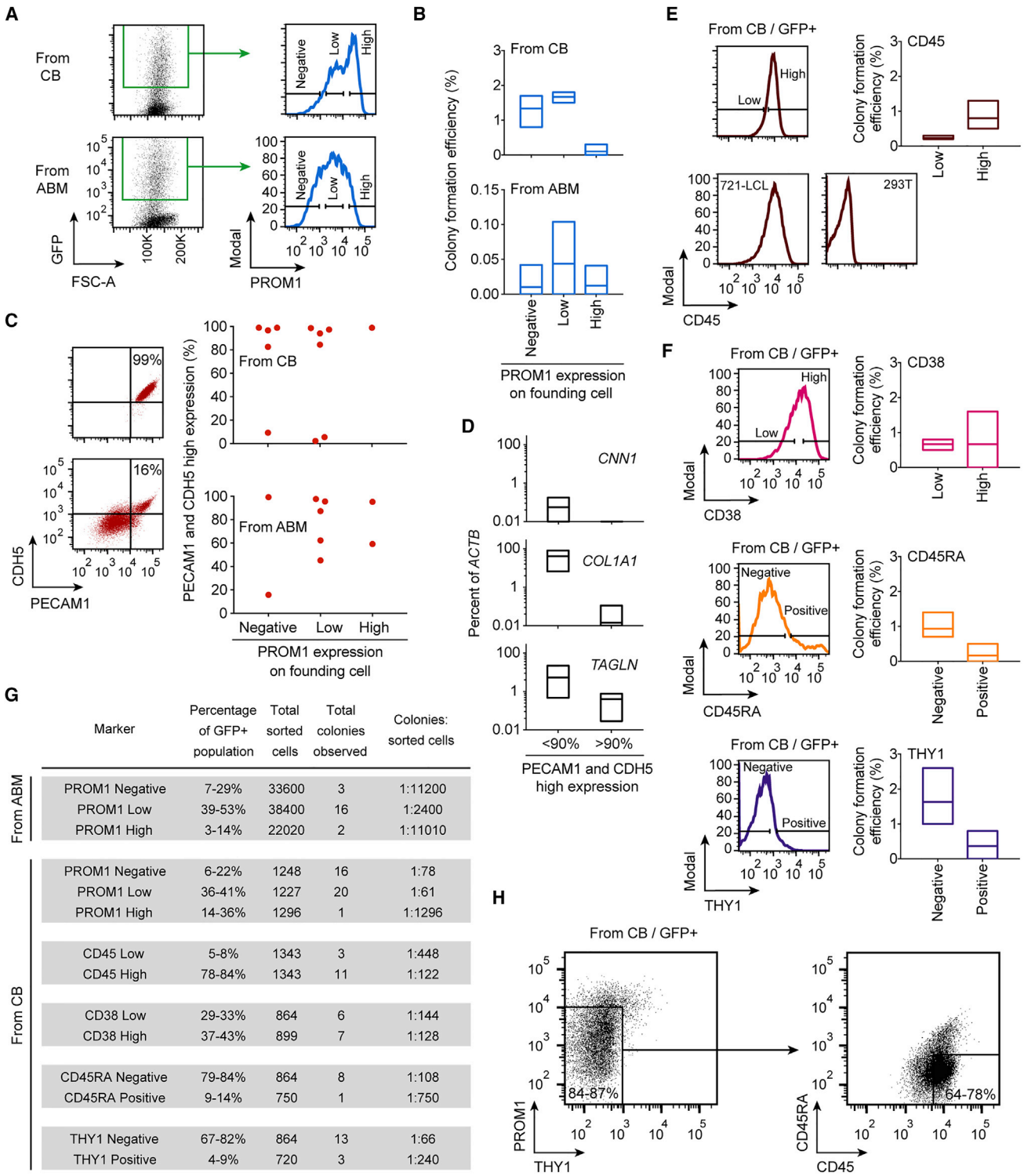

	Marker	Percentage of GFP+ population	Total sorted cells	Total colonies observed	Colonies: sorted cells
From ABM	PROM1 Negative	7-29%	33600	3	1:11200
	PROM1 Low	39-53%	38400	16	1:2400
	PROM1 High	3-14%	22020	2	1:11010
From CB	PROM1 Negative	6-22%	1248	16	1:78
	PROM1 Low	36-41%	1227	20	1:61
	PROM1 High	14-36%	1296	1	1:1296
	CD45 Low	5-8%	1343	3	1:448
	CD45 High	78-84%	1343	11	1:122
	CD38 Low	29-33%	864	6	1:144
	CD38 High	37-43%	899	7	1:128
	CD45RA Negative	79-84%	864	8	1:108
	CD45RA Positive	9-14%	750	1	1:750
	THY1 Negative	67-82%	864	13	1:66
	THY1 Positive	4-9%	720	3	1:240

Figure 5. Investigating the Subpopulations of CD34$^+$ Cells That Give Rise to the eAEPs

(A) CD34$^+$ cells from cord blood (CB) or adult bone marrow (ABM) were electroporated with vectors described in Figure 1 along with a plasmid encoding GFP. Transfected cells (green gate) were isolated by FACS based on their level of expression of PROM1 (negative, low, and high gates). CB cells were sorted into 96-well plates at one cell per well; ABM cells were plated at ten cells per well.

(legend continued on next page)

expression levels correlate best with the cells' ability to resist an EndoMT were identified. By comparing the transcriptomes of resistant eAEPs with permissive eAEPs and eMPs, a small set of genes were elucidated that are either preferentially expressed (15 genes) or depleted (three genes) in resistant cells (Figure 6C). All of these genes except *CD44* (Tang et al., 2012), to our knowledge, have not yet been implicated in the EndoMT; however, *SIM2* has previously been shown to play a role in the related epithelial-to-mesenchymal transition (EMT) (Laffin et al., 2008). The candidate genes include transcriptional regulators (*HOXD4*, *HOXD9*, *SFMBT2*, *SIM2*, *ZNF628*) as well as receptors and adhesion molecules (*ADRA2A*, *CD44*, *FCGR3A*, *IGSF11*, *PPARG*). Next, changes in gene expression that occur as cells relinquish their endothelial identity to become mesenchymal were examined. For this analysis, the correlation between PECAM1 expression and cells undergoing an EndoMT (Figures 3A and 3B) was exploited. The top 50 genes that correlated positively or negatively with PECAM1 were identified and grouped into functional modules: 26 genes involved in cell signaling, 11 genes involved in cell adhesion or the extracellular matrix (ECM), four transcriptional regulators, and three metabolism genes (Figure S6).

DISCUSSION

Using just two transcription factors, *MYCN* and *SOX17*, we are able to induce and propagate in culture human vascular precursors that can give rise to functional arterial endothelial cells. We did not anticipate that the precursors would possess an arterial identity, but, given that *Sox17* is preferentially expressed throughout the arterial system (Liao et al., 2009) and maintains arterial identity in mice (Corada et al., 2013), it was not surprising. In further support for the role of *SOX17*, during the establishment of the cell lines, adherent colonies sometimes appeared in wells with cells transfected with *MYCN* alone after several weeks of culture. It was difficult to isolate individual colonies, but pooled colonies could be propagated. Analysis of marker expression by RNA-seq of these *MYCN*-only cells indicates they do not appreciably express endothelial markers, suggesting that the presence of *SOX17* is central to the arterial endothelial identity in human cells. Our initial notion that *MYCN* and *SOX17* might act as generic tools for expanding blood or vascular cell types was overly simplified; one or both factors supply identity information along with their capacity to propagate cells.

So far, the data indicate that the eAEPs originate from hematopoietic $CD34^+$ cells through rare reprogramming events. Under our experimental conditions, *MYCN* and *SOX17* preferentially induce colonies from cord blood progenitors that are $PROM1^{low/-}THY1^-CD45^{high}CD45RA^-$. This marker profile best fits the marker profile of progenitors that give rise to erythroid and myeloid cells (Doulatov et al., 2010; Gorgens et al., 2013). However, while the majority of transfected cells display the marker profile of erythroid and myeloid progenitors, colony formation is a rare event. Thus, it is not yet clear whether these progenitors themselves, or other rare progenitor(s) that co-mingle with erythroid and myeloid progenitors, are the preferred cells of origin. It is also possible that eAEPs form infrequently because some rate-limiting step (e.g., a particular dosage of *MYCN* or *SOX17* or a particular epigenetic conformation) is required.

Independently derived eAEP lines all share an arterial endothelial phenotype but are not identical. They differ,

(B) Colony formation efficiency of different PROM1 fractions in (A) after 9 days. The boxes indicate the maximum to minimum efficiencies from three (CB) and five (ABM) independent experiments; the horizontal lines within the boxes indicate the means.
(C) Analysis of expanded colonies from (B) by flow cytometry for the expression of the endothelial markers CDH5 and PECAM1. The CB colonies are from one lot of $CD34^+$ cells, the ABM colonies are from three different lots. Cells were expanded for 49 days from the induction of the ectopic expression of *MYCN* and *SOX17* and then matured by the withdrawal of doxycycline for an additional 4 days. Left, example dot plots. The double-positive gate used here identifies cells with high expression of CDH5 and PECAM1. Right, compilation of the results from flow cytometry.
(D) Measurements by RT-qPCR of the expression levels of mesenchymal markers from the cells in (C). The boxes indicate the maximum to minimum values; the horizontal lines within the boxes indicate the means. Values are normalized as a percentage of *ACTB* and presented on a $\log_{10}$ scale, with a threshold of detection cutoff of 0.01%.
(E and F) $CD34^+$ cells from cord blood were electroporated as in (A); transfected cells (GFP^+) were isolated by FACS based on the indicated level of expression of each marker. Cells were sorted into 96-well plates at one cell per well. The example histograms are of cells gated for expression of GFP as in (A). The colony formation efficiency of each fraction was determined in three independent experiments as described in (B). (E) Cells sorted based on their level of expression of CD45. 721-LCL (lymphoblastoid) cells served as positive controls; 293T cells served as negative controls. (F) Cells sorted based on their level of expression of CD38, CD45RA, or THY1.
(G) Additional summary statistics from the experiments described in (A, B, E, F).
(H) $CD34^+$ cells from cord blood were transfected as described in (A) and then analyzed by flow cytometry. The example dot plots are of cells gated for expression of GFP as in (A). The minimum to maximum percentages of cells within each gate as measured in three independent experiments are indicated.

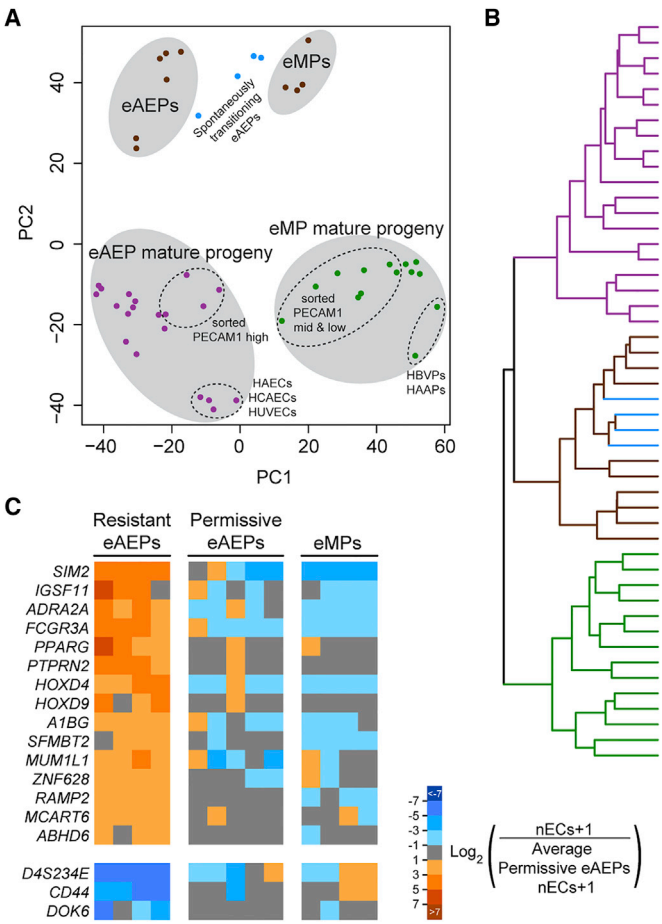

Figure 6. eAEPs and eMPs Form a Distinct Transcriptional Topography That Reveals Insights into the EndoMT

(A and B) The transcriptomes of cells were measured by RNA-seq. In prior figures, select portions of the transcriptomes are presented. Here, the transcriptomes were more broadly evaluated. The eAEPs or eMPs were maintained with at least 100 ng/mL doxycycline. The mature progeny of the eAEPs or eMPs were obtained by cultivation in the presence of 0 or 10 ng/mL doxycycline for 4 (eAEPs) or 3 (eMPs) days. Sorted PECAM1 high, mid, and low indicate cells isolated by FACS from lines spontaneously undergoing an EndoMT (Figure 3B). (A) Principal component analysis. (B) Unsupervised hierarchical clustering. HAAFs, human aortic adventitial fibroblasts; HAECs, human aortic endothelial cells; HBVPs, human brain vascular pericytes; HCAECs, human coronary artery endothelial cells; HUVECs, human umbilical vein endothelial cells.

(C) Genes that are preferentially expressed or depleted in EndoMT-resistant eAEPs. The genes were identified by comparing the transcriptomes of EndoMT-resistant eAEPs with EndoMT-permissive eAEPs and eMPs using RNA-seq samples presented in prior figures. nECs, normalized expected counts. The heatmap is depicted on $\log_2$ scale, using the average expression values (nECs + 1) of the EndoMT-permissive eAEPs as the baseline for comparison. See Supplemental Experimental Procedures for more detail. See also Figure S6.

for example, in the efficiency by which they construct lumenized tubes or by the amount of wall shear stress required to best align them with the direction of fluid flow. We view the differences between the cell lines as a unique asset; they fortuitously provide a wealth of phenotypes that can be tractably studied to aid our understanding of basic biological phenomena as well as pathological dysfunction. In this study, we explored the differences in the ability of cells to undergo an EndoMT, a process that is implicated in a wide array of vascular diseases and disorders. Over time in culture, some cell lines readily convert to a mesenchymal state (EndoMT permissive), while others resist this transition for longer (EndoMT resistant). These distinctions can be exacerbated by a blockade of FGF signaling or, to a much lesser extent, by exposure to TGF-β. Furthermore, some cell lines (eMPs) appear to rapidly become mostly mesenchymal during their initial establishment in culture. An analysis of cells spontaneously undergoing an EndoMT revealed transcriptome-wide changes in genes involved in cell signaling, ECM, adhesion, transcription, and metabolism. A number of these alterations may have roles in vascular dysfunction. For example, both *NPR3* and *ITGB2*, which strongly increase as cells transition, have previously been shown to be upregulated in atherosclerotic plaques of carotid arteries (Di Taranto et al., 2012; Zayed et al., 2016). The transitioned cells appear poised to extensively remodel their environment; collagen I (*COL1A1*, *COL1A2*) is upregulated along with a cohort of other ECM proteins including *COL5A3*, *COL6A3*, *FN1*, and *KRT81*. The transitioned cells also likely emit signals distinct from surrounding endothelium; they preferentially express the growth factor *GDF6* (*BMP13*) and growth factor binding protein *IGFBP6* while downregulating the growth factor *PGF*.

The spontaneous transition in culture from an endothelial identity toward a mesenchymal one occurs over time. The permissive lines can exhibit transitioned cells within several months in culture; the resistant lines take much longer. It remains unclear what prompts the cells to spontaneously transition and whether the event is clonal or

polyclonal. Perhaps some mesenchymal states are more suited to cell culture, providing any cell that transitions with a selective advantage. In support of this notion, eMPs exhibit a normal karyotype and some can expand faster than eAEPs. It is possible that the resistant lines can only access a less expandable mesenchymal state (as exemplified by the eMP line MS51), and thus any spontaneously transitioning cells in these lines are not endowed with a selective advantage in culture. When an EndoMT is exacerbated by a blockade of FGF signaling, the efficiency of transition seems to increase. Even the resistant lines move toward a mesenchymal state but rebound if the blockade is lifted after 4 days. Their capacity to rebound seems to decline after extensive passaging, indicating that their higher threshold of commitment to the mesenchymal state slowly lowers over time in culture.

Because the expression of the marker PROM1 varies substantially among $CD34^+$ cells, we examined whether or not PROM1 levels are indicative of the capacity of the cells to give rise to EndoMT-permissive or -resistant eAEPs. In $CD34^+$ cells derived from cord blood, those with low or undetected levels of PROM1 had a greater capacity to form eAEPs, but this result was not recapitulated well in cells derived from adult bone marrow. In addition, both EndoMT-permissive and -resistant eAEPs could be obtained from $CD34^+$ progenitors of each fraction of PROM1 expression, indicating that this parameter does not correlate with proclivity to an EndoMT.

What factors might endow cells with the ability to resist an EndoMT? The differences do not seem to correlate well with the levels of *MYCN* or *SOX17* and probably reflect epigenetic or genetic differences between the founding $CD34^+$ cells. The resistant cell lines preferentially express or repress a small set of genes compared with permissive or mostly mesenchymal cell lines, and most of these genes have not been implicated in an EndoMT to our knowledge. A number of the genes preferentially expressed in resistant cells are transcription factors, one or more of which perhaps function to impose the higher threshold of commitment to the mesenchymal state observed in these cells. Although our sample size is small, the most resistant cell lines (MS53 and MS55) are derived from bone marrow. If this trend holds, it may indicate that different reservoirs of $CD34^+$ progenitors possess distinct vascular properties.

It is also worth pointing out that we observe cells undergoing an EndoMT in the precursor state, before the cells mature. If the precursors induced and expanded by *MYCN* and *SOX17* faithfully mimic their vascular counterparts *in vivo*, this observation raises the possibility that resident or circulating vascular progenitors may alter their identity as a result of environmental changes or age. For example, the number of circulating cells expressing both KDR and CD34 (a population of cells thought to be enriched for endothelial progenitors) declines significantly in individuals with vascular disease who go on to have a major cardiovascular event (Schmidt-Lucke et al., 2005; Werner et al., 2005). Since we detect the loss of *KDR* and/or *CD34* expression in transitioning cells (Figure 3), perhaps the number of progenitors appears to decline because the cells have converted to a mesenchymal precursor state. Given their proliferative capacity, such transitioned vascular progenitors may well be important drivers of the progression of cardiovascular disease.

EXPERIMENTAL PROCEDURES

Expression Vectors

All integrating vectors used were based on the PiggyBac transposon system and are akin to previously described vectors (Vereide et al., 2014). The open reading frames for human *MYCN* or *SOX17* (Genecoepia) were introduced into a PiggyBac vector downstream of the doxycycline-inducible promoter TRE3G (Clontech). A cassette encoding the doxycycline-responsive transactivator *Tet-On 3G* (expressed by the constitutively active elongation factor 1 alpha (EF1α) promoter, Clontech) was also introduced into a PiggyBac vector. The plasmid pmaxGFP (Lonza) was used in experiments described in Figure 5 as a means to transiently label transfected cells.

Sources of Primary Cells

Frozen primary $CD34^+$ cells purified from umbilical cord blood or adult bone marrow were obtained from AllCells (for cord blood, products CB005F and CB009F; for adult bone marrow, product ABM022F). Human umbilical vein endothelial cells (HUVECs), human aortic endothelial cells (HAECs), and human coronary artery endothelial cells (HCAECs) were obtained from Lonza.

ACCESSION NUMBERS

The accession number for the RNA-seq data reported in this paper is GEO: GSE106991.

SUPPLEMENTAL INFORMATION

Supplemental Information includes Supplemental Experimental Procedures, six figures, and one table and can be found with this article online at https://doi.org/10.1016/j.stemcr.2017.12.011.

AUTHOR CONTRIBUTIONS

D.T.V. designed, conducted, and analyzed experiments and wrote the manuscript. A.Z.M., A.S., A.P.T., and A.N. assisted D.T.V. in conducting and analyzing experiments and editing the manuscript. J.A.T. provided facilities, personnel, and reagents for the RNA-seq experiments.

ACKNOWLEDGMENTS

This work was supported by a fellowship to D.T.V. from the Morgridge Institute for Research and NHLBI grant U01HL134655 to J.A.T. We thank Wendy Vardaman for illustrations in Figure 1;

Danny Mamott and Mitch Probasco for assistance sorting cells by FACS; Cara Argus, Jen Bolin, Angela Elwell, and Matt Schmitz for the preparation and sequencing of the RNA-seq samples; and Scott Swanson and John Steill for processing the RNA-seq data (Casava through RSEM steps). We thank Vernella Vickerman, Li-Fang Chu, and Jue Zhang for helpful discussions and Patrick Ingram, David Porkka, and Erin Syth for critically reading drafts of the manuscript.

Received: September 6, 2016
Revised: December 13, 2017
Accepted: December 14, 2017
Published: January 9, 2018

REFERENCES

Aird, W.C. (2005). Spatial and temporal dynamics of the endothelium. J. Thromb. Haemost. *3*, 1392–1406.

Aird, W.C. (2007). Phenotypic heterogeneity of the endothelium: I. Structure, function, and mechanisms. Circ. Res. *100*, 158–173.

Chen, P.Y., Qin, L., Baeyens, N., Li, G., Afolabi, T., Budatha, M., Tellides, G., Schwartz, M.A., and Simons, M. (2015). Endothelial-to-mesenchymal transition drives atherosclerosis progression. J. Clin. Invest. *125*, 4514–4528.

Cheng, C., Helderman, F., Tempel, D., Segers, D., Hierck, B., Poelmann, R., van Tol, A., Duncker, D.J., Robbers-Visser, D., Ursem, N.T., et al. (2007). Large variations in absolute wall shear stress levels within one species and between species. Atherosclerosis *195*, 225–235.

Cheng, C.P., Herfkens, R.J., and Taylor, C.A. (2003). Abdominal aortic hemodynamic conditions in healthy subjects aged 50-70 at rest and during lower limb exercise: in vivo quantification using MRI. Atherosclerosis *168*, 323–331.

Cicinelli, E., Ignarro, L.J., Schonauer, L.M., Matteo, M.G., Galantino, P., and Falco, N. (1999). Different plasma levels of nitric oxide in arterial and venous blood. Clin. Physiol. *19*, 440–442.

Cooley, B.C., Nevado, J., Mellad, J., Yang, D., St Hilaire, C., Negro, A., Fang, F., Chen, G., San, H., Walts, A.D., et al. (2014). TGF-beta signaling mediates endothelial-to-mesenchymal transition (EndMT) during vein graft remodeling. Sci. Transl. Med. *6*, 227ra234.

Corada, M., Orsenigo, F., Morini, M.F., Pitulescu, M.E., Bhat, G., Nyqvist, D., Breviario, F., Conti, V., Briot, A., Iruela-Arispe, M.L., et al. (2013). Sox17 is indispensable for acquisition and maintenance of arterial identity. Nat. Commun. *4*, 2609.

Di Taranto, M.D., Morgante, A., Bracale, U.M., D'Armiento, F.P., Porcellini, M., Bracale, G., Fortunato, G., and Salvatore, F. (2012). Altered expression of inflammation-related genes in human carotid atherosclerotic plaques. Atherosclerosis *220*, 93–101.

Doulatov, S., Notta, F., Eppert, K., Nguyen, L.T., Ohashi, P.S., and Dick, J.E. (2010). Revised map of the human progenitor hierarchy shows the origin of macrophages and dendritic cells in early lymphoid development. Nat. Immunol. *11*, 585–593.

Durr, E., Yu, J., Krasinska, K.M., Carver, L.A., Yates, J.R., Testa, J.E., Oh, P., and Schnitzer, J.E. (2004). Direct proteomic mapping of the lung microvascular endothelial cell surface in vivo and in cell culture. Nat. Biotechnol. *22*, 985–992.

Fishbein, M.C., and Fishbein, G.A. (2015). Arteriosclerosis: facts and fancy. Cardiovasc. Pathol. *24*, 335–342.

Goligorsky, M.S., and Salven, P. (2013). Concise review: endothelial stem and progenitor cells and their habitats. Stem Cells Transl. Med. *2*, 499–504.

Gorgens, A., Radtke, S., Mollmann, M., Cross, M., Durig, J., Horn, P.A., and Giebel, B. (2013). Revision of the human hematopoietic tree: granulocyte subtypes derive from distinct hematopoietic lineages. Cell Rep. *3*, 1539–1552.

Hauser, I.A., Johnson, D.R., and Madri, J.A. (1993). Differential induction of VCAM-1 on human iliac venous and arterial endothelial cells and its role in adhesion. J. Immunol. *151*, 5172–5185.

Kokudo, T., Suzuki, Y., Yoshimatsu, Y., Yamazaki, T., Watabe, T., and Miyazono, K. (2008). Snail is required for TGFbeta-induced endothelial-mesenchymal transition of embryonic stem cell-derived endothelial cells. J. Cell Sci. *121*, 3317–3324.

Kovacic, J.C., Moore, J., Herbert, A., Ma, D., Boehm, M., and Graham, R.M. (2008). Endothelial progenitor cells, angioblasts, and angiogenesis–old terms reconsidered from a current perspective. Trends Cardiovasc. Med. *18*, 45–51.

Lacorre, D.A., Baekkevold, E.S., Garrido, I., Brandtzaeg, P., Haraldsen, G., Amalric, F., and Girard, J.P. (2004). Plasticity of endothelial cells: rapid dedifferentiation of freshly isolated high endothelial venule endothelial cells outside the lymphoid tissue microenvironment. Blood *103*, 4164–4172.

Laffin, B., Wellberg, E., Kwak, H.I., Burghardt, R.C., Metz, R.P., Gustafson, T., Schedin, P., and Porter, W.W. (2008). Loss of singleminded-2s in the mouse mammary gland induces an epithelial-mesenchymal transition associated with up-regulation of slug and matrix metalloprotease 2. Mol. Cell. Biol. *28*, 1936–1946.

Liao, W.P., Uetzmann, L., Burtscher, I., and Lickert, H. (2009). Generation of a mouse line expressing Sox17-driven Cre recombinase with specific activity in arteries. Genesis *47*, 476–483.

Lozano, R., Naghavi, M., Foreman, K., Lim, S., Shibuya, K., Aboyans, V., Abraham, J., Adair, T., Aggarwal, R., Ahn, S.Y., et al. (2012). Global and regional mortality from 235 causes of death for 20 age groups in 1990 and 2010: a systematic analysis for the Global Burden of Disease Study 2010. Lancet *380*, 2095–2128.

Piera-Velazquez, S., Li, Z., and Jimenez, S.A. (2011). Role of endothelial-mesenchymal transition (EndoMT) in the pathogenesis of fibrotic disorders. Am. J. Pathol. *179*, 1074–1080.

Schmidt-Lucke, C., Rossig, L., Fichtlscherer, S., Vasa, M., Britten, M., Kamper, U., Dimmeler, S., and Zeiher, A.M. (2005). Reduced number of circulating endothelial progenitor cells predicts future cardiovascular events: proof of concept for the clinical importance of endogenous vascular repair. Circulation *111*, 2981–2987.

Stenmark, K.R., Yeager, M.E., El Kasmi, K.C., Nozik-Grayck, E., Gerasimovskaya, E.V., Li, M., Riddle, S.R., and Frid, M.G. (2013). The adventitia: essential regulator of vascular wall structure and function. Annu. Rev. Physiol. *75*, 23–47.

Tang, R., Gao, M., Wu, M., Liu, H., Zhang, X., and Liu, B. (2012). High glucose mediates endothelial-to-chondrocyte transition in human aortic endothelial cells. Cardiovasc. Diabetol. *11*, 113.

Thompson, R.C., Allam, A.H., Lombardi, G.P., Wann, L.S., Sutherland, M.L., Sutherland, J.D., Soliman, M.A., Frohlich, B., Mininberg, D.T., Monge, J.M., et al. (2013). Atherosclerosis across 4000 years of human history: the Horus study of four ancient populations. Lancet *381*, 1211–1222.

Vereide, D.T., Vickerman, V., Swanson, S.A., Chu, L.F., McIntosh, B.E., and Thomson, J.A. (2014). An expandable, inducible hemangioblast state regulated by fibroblast growth factor. Stem Cell Rep. *3*, 1043–1057.

Werner, N., Kosiol, S., Schiegl, T., Ahlers, P., Walenta, K., Link, A., Bohm, M., and Nickenig, G. (2005). Circulating endothelial progenitor cells and cardiovascular outcomes. N. Engl. J. Med. *353*, 999–1007.

Zayed, M.A., Harring, S.D., Abendschein, D.R., Vemuri, C., Lu, D., Detering, L., Liu, Y., and Woodard, P.K. (2016). Natriuretic peptide Receptor-C is up-regulated in the intima of advanced carotid artery atherosclerosis. J. Med. Surg. Pathol. *1*, 131.

Zhang, J., Chu, L.F., Hou, Z., Schwartz, M.P., Hacker, T., Vickerman, V., Swanson, S., Leng, N., Nguyen, B.K., Elwell, A., et al. (2017). Functional characterization of human pluripotent stem cell-derived arterial endothelial cells. Proc. Natl. Acad. Sci. USA *114*, E6072–E6078.